Supporting for

Revisiting Pt/TiO_2 photocatalyst in the thermally assisted photocatalytic reduction of CO_2

Fei Yu[a], Changhua Wang[a]*, He Ma[a], Miao Song[b], Dongsheng Li[b], Yingying Li[a], Songmei Li[a], Xintong Zhang[a]* and Yichun Liu[a]

[a] Key Laboratory of UV-Emitting Materials and Technology of Chinese Ministry of Education, Northeast Normal University, 5268 Renmin Street, Changchun 130024, China

[b] Physical and Computational Sciences Directorate, Pacific Northwest National Laboratory, Richland, WA, 99352, United States

* Corresponding authors: wangch100@nenu.edu.cn; xtzhang@nenu.edu.cn

1. Experiment

1.1. Material synthesis.

Firstly, 0.8 mL titanium tetrachloride ($TiCl_4$), 5 mL $NH_3 \cdot H_2O$ (25%), 10 mL H_2O_2 (30%) and 0.5 g glycolic acid were added into 45 mL ice water with magnetic stirring. The mixed solution was then heated at 80 °C for 390 mins and a yellowish gel was formed ultimately. Deionized water was added to dissolve the gel, the pH of the solution was adjusted to 2 by H_2SO_4. In this step, the total volume of solution was set at 50 mL. Finally, the solution was separated into two equal parts, which were sealed respectively in a 50 mL autoclave and heated at 160 °C for 50 min. After reaction, the sample was centrifugated and washed with ethanol and deionized water for several times and then dried at 80 °C in the oven. The collected product was calcined at 370 °C for 1 h. Since the product is composed by anatase and TiO_2(B) , as proven by XRD and Raman characterization, the as-obtained sample was named as AB for simplicity.

1.2. Material Characterization.

UV−vis diffuse reflectance (DR) spectra of the samples were collected on a PerkinElmer UV WinLab spectrophotometer, and $BaSO_4$ was used as a reference. The crystal structure and phase identification were characterized by X-ray diffraction (XRD, Rigaku, D/max-2500 X-ray diffractometer) using Cu Kα radiation (λ = 1.5406Å). Raman spectra used J-Y UV-lamb micro-Raman spectrometer under an excitation of a 488 nm Ar^+ laser. The morphology of the samples was characterized with a transmission electron microscope (TEM, a JEM-2100 transmission electron microscope) at an acceleration voltage of 200 kV. High-resolution TEM (HRTEM) images were obtained with a JEOL JEM 2100F TEM at an accelerating voltage of 200 kV. High-angle annular dark-field scanning transmission electron microscopy(HAADF-STEM) and elemental mapping, images were acquired by energy dispersive X-ray spectroscopy (EDS) using a JEOL-2100F electron microscope equipped with a STEM unit. X-ray photoelectron spectroscopy (XPS) experiments were performed on a Thermo SCIENTIFIC ESCALAB 250Xi instrument with an Al Kα ADES (hν =1486.8eV).

1.3. Photoelectrochemical measurements.

Photoelectrochemical measurements were performed on Princeton 2273 electrochemical work-station with a standard three-electrode configuration in 1M NaOH aqueous solution. A platinum plate and Ag/AgCl were used as the counter and reference electrode, respectively. The electrolyte was 3.5 M KCl. The working electrodes were prepared as following: 0.05 g of samples were ultrasonic dispersed in 4 mL ethanol for 10 min. The powder suspension was spin-coated onto 2.5 × 1.25 cm^2 FTO substrate. The speed and continuous time were set at 2000 r/min and 10 s, respectively. Each spin coating was performed by dipping 50 μL suspension onto FTO with an active area about of 1.62 cm^2 and repeated for 20 layers. The as-coated films were annealed at 300 ^oC for 30 min. The light intensity illuminated on the samples was 100 mW/cm^2 using the simulated solar irradiation.

1.4. Density functional theory calculations

The DFT calculations were implemented using the plane wave electronic structure code denoted as the Vienna ab initio Simulation Package (VASP). Specifically, the exchange-correlation functional in the Perdew-Burke-Ernzerhof (PBE) form was adopted within a generalized gradient approximation (GGA). The on-site coulomb interactions (U) of the localized 3d electrons of Ti were investigated using the DFT + U method with $U - J = 8$ eV, where J represents the on-site exchange interactions. The (001) surface of TiO_2(A) and the (100) surface of TiO_2(B) were modeled by supercells containing eight atomic layers and a vacuum layer of 20 Å to prevent interactions between the periodic images. In addition, the interface between TiO_2(A) and TiO_2(B) was modeled by a supercell containing six atomic layers on both sides of the interface along with a 20 Å vacuum layer. The kinetic energy cut off was set as 500 eV. A total energy convergence criterion of 10^{-4} eV between two electronic steps was adopted. The Brillouin zones of TiO_2(A) and TiO_2(B) were sampled by k-point meshes with dimensions 10 × 10 × 4 and 4 × 12 × 6, respectively. A k-point mesh with dimensions 6 × 6 × 1 was employed for both surface and interface calculations.

Ionic relaxations were conducted under the force convergence criteria (0.05 eV/Å).

1.5. CO_2 reduction measurements

Photocatalytic (PC) and photothermal catalytic (PTC) induced CO_2 reduction processes were conducted with CO_2 and H_2O under simulated solar light irradiation for 5 h at 298 K and 393 K, respectively. The photocatalysts included TiO_{2-x} and D-TiO_{2-x}, both before and after Pt photodeposition. The experiments were conducted in a stainless-steel autoclave reactor (100 mL) with a quartz viewing window at the top. Continuous full spectrum radiation was provided with an intensity of 100 mW cm^{-2} by a Hayashi LA-410 Xe lamp (150 W). Firstly, 20 mg of a given photocatalyst was ultrasonically dispersed in 2 mL of deionized water and placed in the reactor. Then, the autoclave was sealed and the internal atmosphere was degassed quickly and completely by the introduction of high-purity CO_2 (99.999% with no other carbon-containing compounds detected) for 20 min at room temperature and atmospheric pressure. All tests were conducted with a CO_2 partial pressure of 0.1 MPa. The gaseous mixtures generated in the CO_2 reduction processes were analyzed using a Shimadzu 2014C GC gas chromatograph. Based on these results, we determined the CO, CH_4, and H_2 yields ($\mu mol \cdot h^{-1}$), and calculated the electron reaction rate (*ERR*) as $ERR = 2r(H_2) + 8r(CH_4) + 2r(CO)$, where r is an empirical rate constant. In addition, the CH_4 selectivity was obtained as $\{[8r(CH_4)]/[ERR]\} \times 100\%$. This represents a clear definition of CH_4 selectivity that accounts for the effect of H_2 generated from H_2O in the CO_2 conversion process.

Table S1 Comparison of the selectivity of CH_4 over different semiconductor catalysts with oxygen vacancies (V_O) in photoreduction CO_2.

Catalyst	Light source	Reaction Condition	CH_4 rate (μmol $g^{-1}h^{-1}$)	Selectivity of CH_4	Products
[1] TiO_2-V_O	UV light	393 K, 50 mg cat., 1.33 bar CO_2, 2 mL H_2O	0.4829	**12.63%**	CH_4, CO
[2] TiO_2-V_O	Solar light	50 mg cat., 2 bar CO_2, 6 mL H_2O	16.2	**79.00%**	CH_4, CO, H_2
[2] TiO_2-V_O	Visible light	50 mg cat., 2 bar CO_2, 6 mL H_2O	2.7	**73.00%**	CH_4, CO, H_2
[3] TiO_2-V_O	Solar light	50 mg cat., 2 bar CO_2, mL H_2O	14.3	**74.00%**	CH_4, CO, H_2
[4] WO_3-V_O	Visible light	523 K, 50 mg cat., 25 kPa CO_2, H_2O	1.042	**41.00%**	CH_4, CH_3OH
[5]BiOCl-V_O	Solar light	50 mg cat., 400 ppm CO_2, 100 mL H_2O	0.144	**36.50%**	CH_4, CO

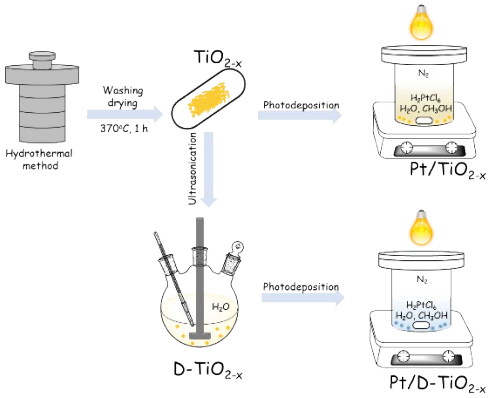

Scheme S1 Fabrication processes of the TiO_{2-x}, surface disordered TiO_{2-x} (D-TiO_{2-x}), Pt/TiO_{2-x}, and Pt/D-TiO_{2-x} photocatalysts.

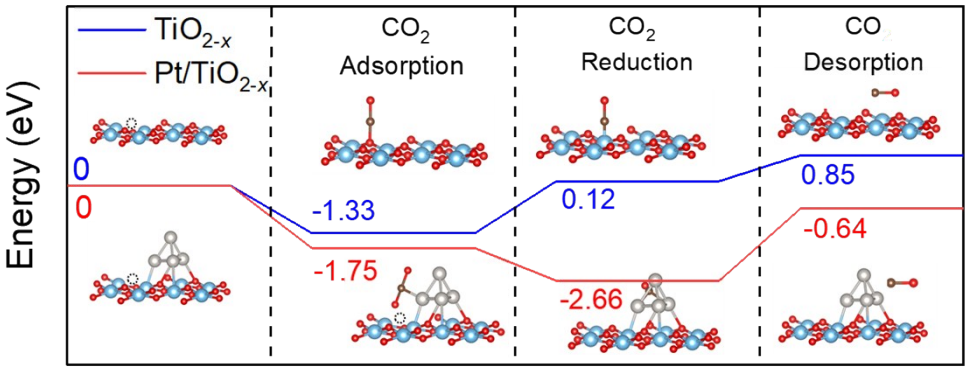

Fig. S1 Whole reaction process of TiO_{2-x} and Pt-loaded TiO_{2-x}.

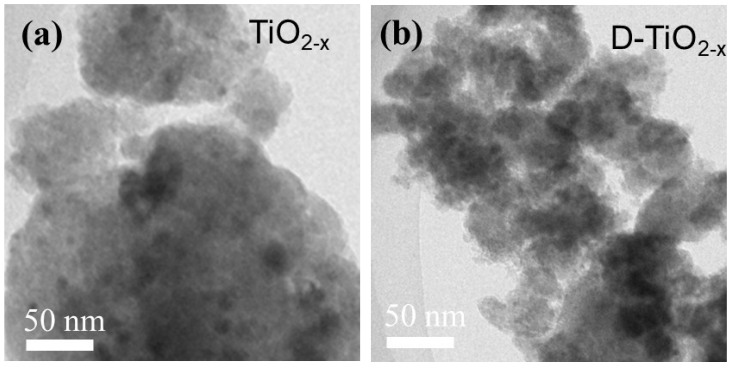

Fig. S2 TEM images of (a) TiO_{2-x} and (b) D-TiO_{2-x}.

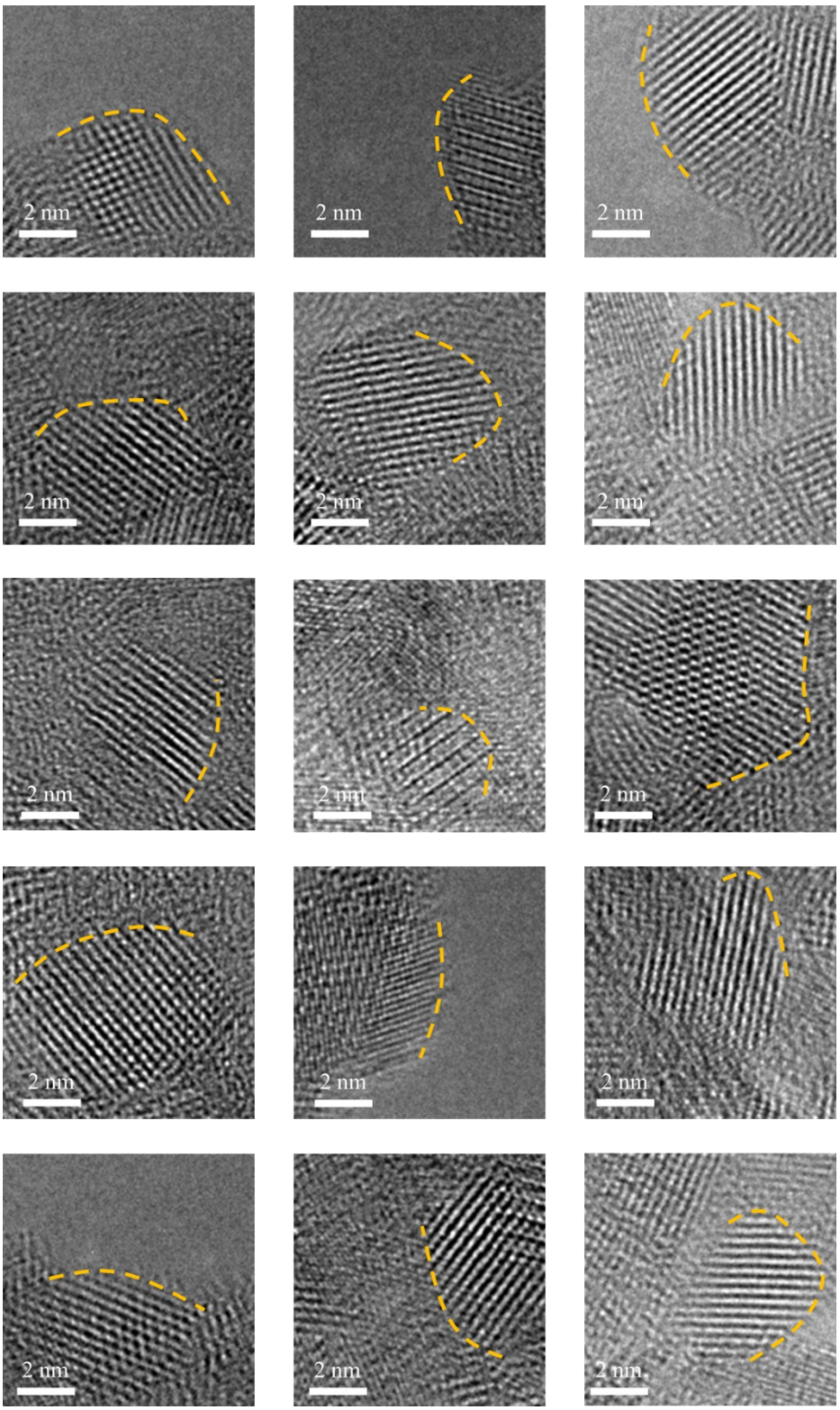

Fig. S3 HRTEM images of the TiO_{2-x}.

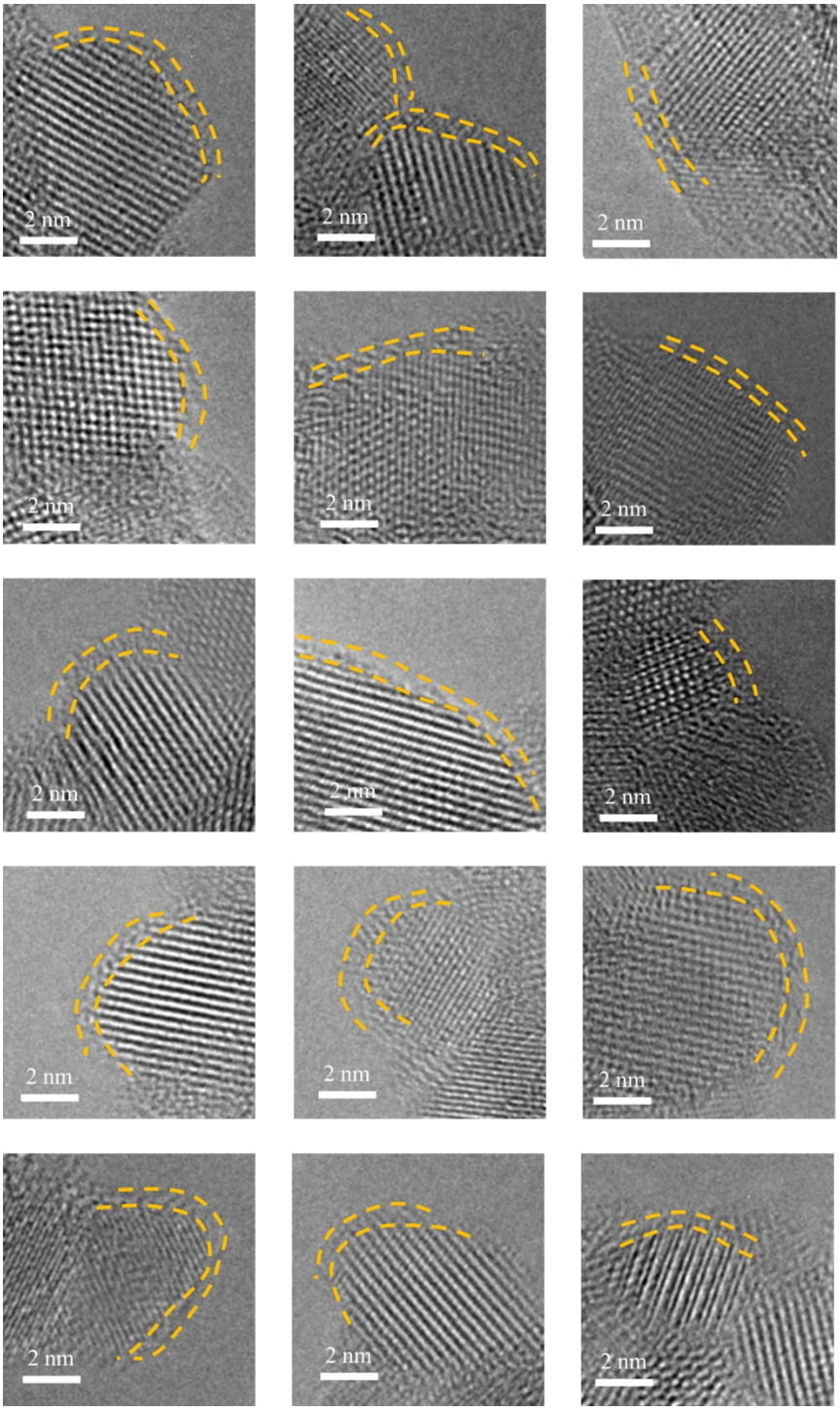

Fig. S4 HRTEM images of the D-TiO_{2-x}.

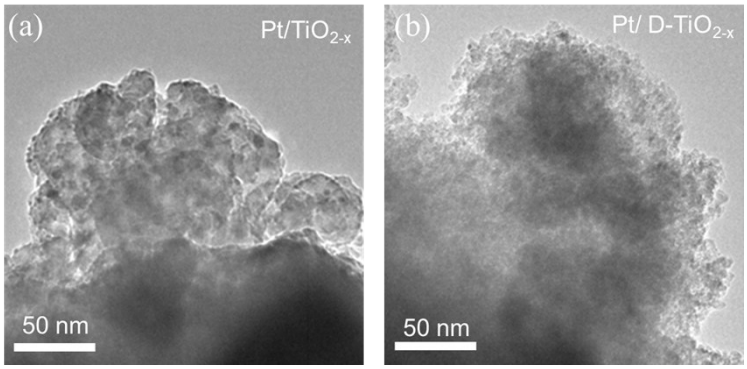

Fig. S5 TEM images of Pt/TiO_{2-x} and Pt/D-TiO_{2-x}

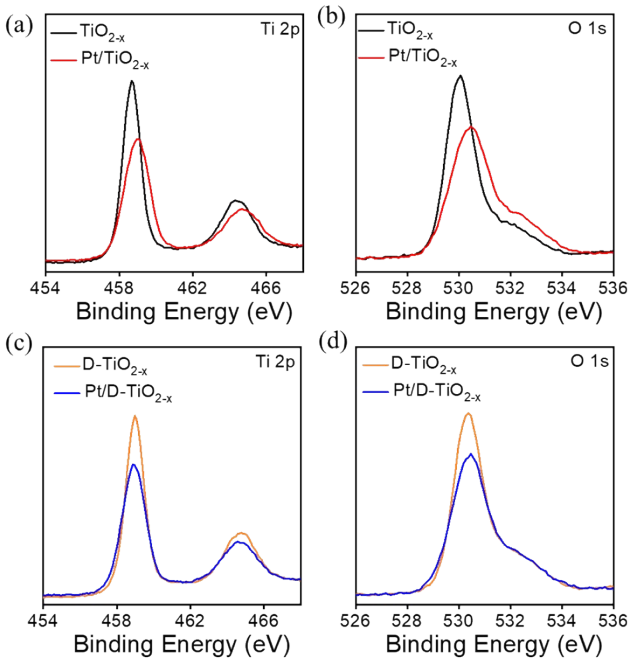

Fig. S6 XPS spectra of (a) Ti 2p and (b) O 1s score level of TiO_{2-x} and Pt/TiO_{2-x}; XPS spectra of (c) Ti 2p and (d) O 1s score level of D-TiO_{2-x} and Pt/D-TiO_{2-x}.

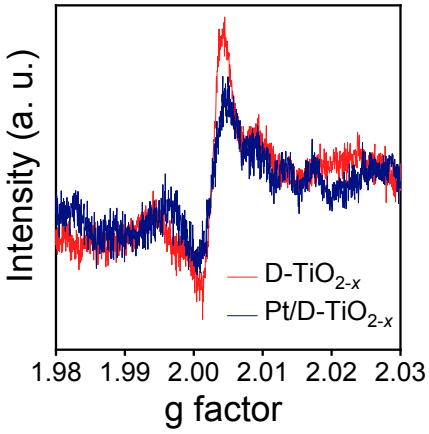

Fig. S7 ESR spectra of Pt/TiO_{2-x} and Pt/D-TiO_{2-x}.

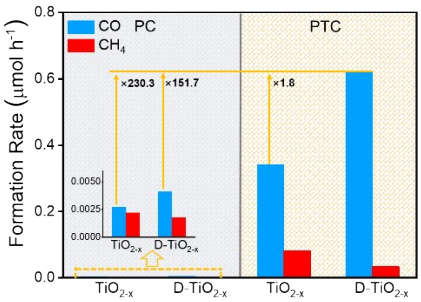

Fig. S8 Photocatalytic (PC) and photothermal catalytic (PTC) induced CO_2 to CO conversion using TiO_{2-x} and D-TiO_{2-x} photocatalysts.

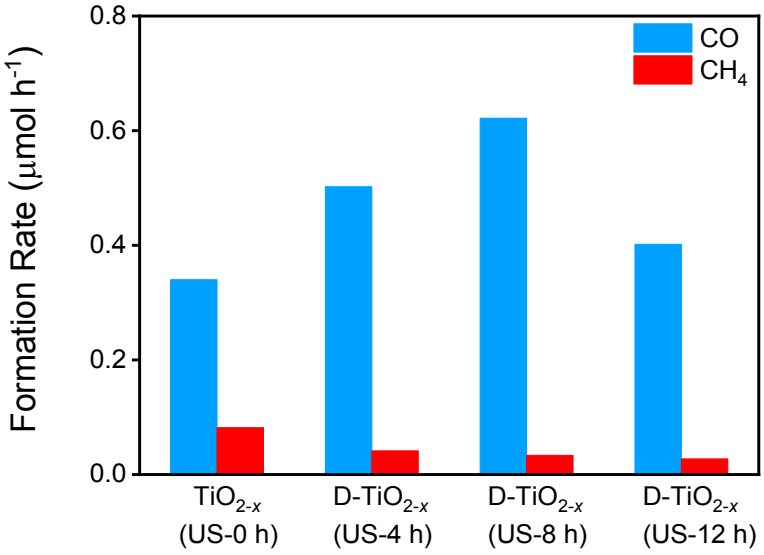

Fig. S9 Photothermal catalytic (PTC) induced CO_2 to CO conversion using TiO_{2-x} treated by ultrasonication for different time.

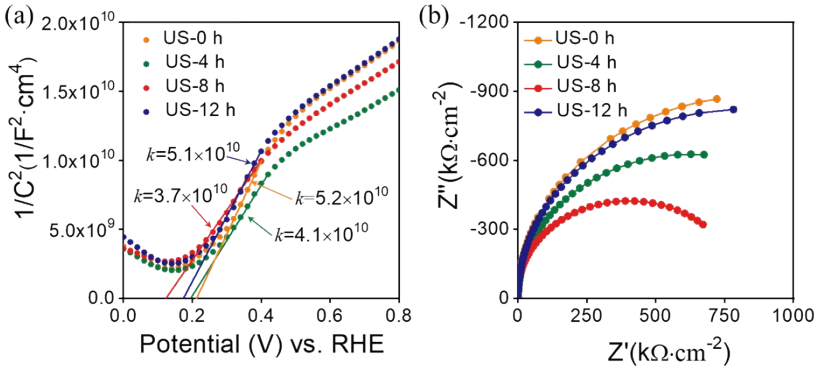

Fig. S10 Characterizations of the US-X photocatalysts: (a) Mott-Schottky plots obtained at a frequency of 1 kHz in the absence of incident light; (b) Nyquist plots obtained under illumination with a 1 M NaOH electrolyte at a DC potential of 1.23 V relative to a reversible hydrogen electrode (RHE) and an AC voltage amplitude of 10 mV with frequencies ranging from 100 kHz to 0.01 Hz, where the inset presents the equivalent circuit model employed during analysis.

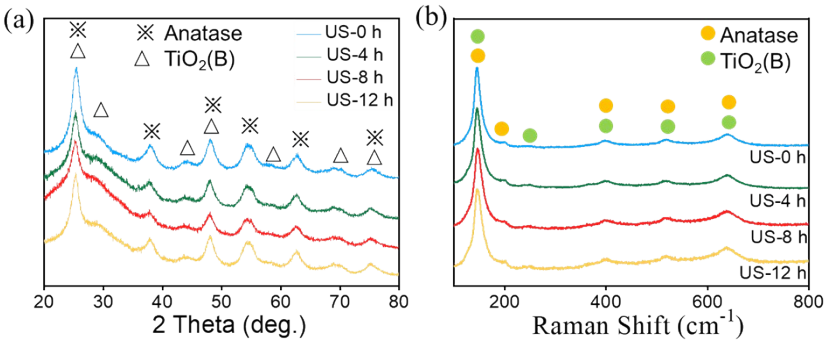

Fig. S11 Characterizations of the US-X photocatalysts: (a) XRD patterns; (b) Raman spectra.

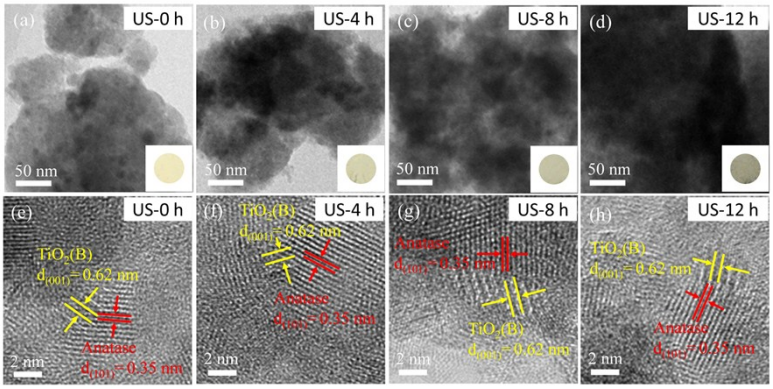

Fig. S12 TEM and HRTEM images of (a) and (e) US-0 h, (b) and (f) US-4h, (e) and (g) US-8 h, (d) and (h) US-12.

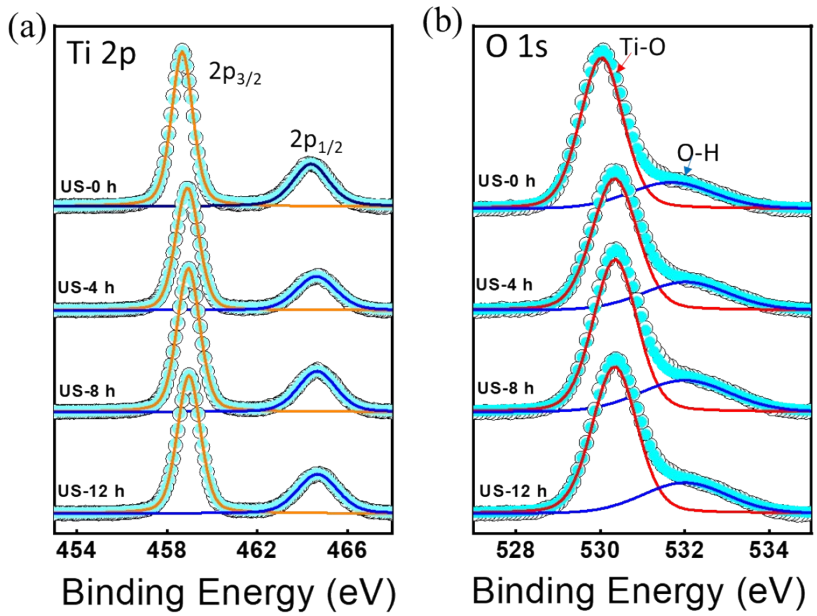

Fig. S13 XPS spectra of (a) Ti 2p and (b) O 1s score level of US-X.

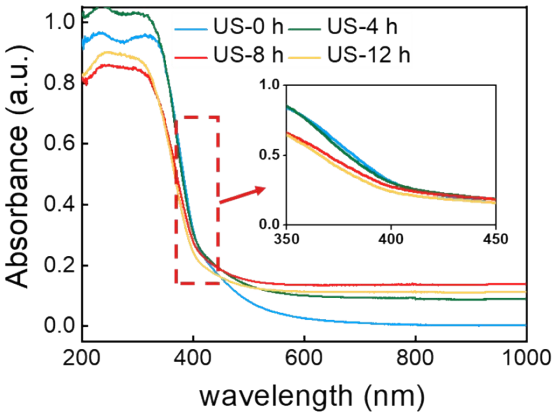

Fig. S14 The ultraviolet-visible absorption spectra of US-X.

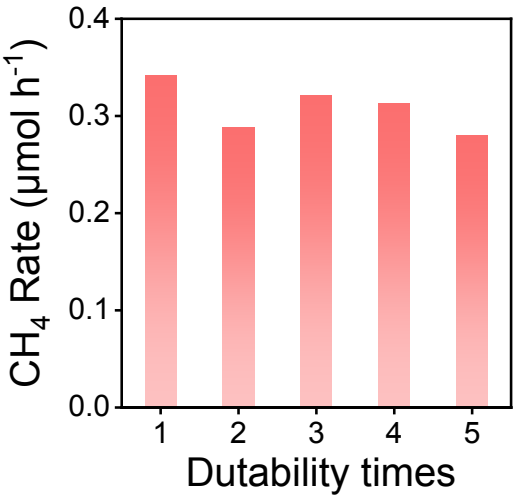

Fig. S15 Recycling of Pt/D-TiO_{2-x} catalyst for CH_4 formation via photothermal catalytic reduction of CO_2.

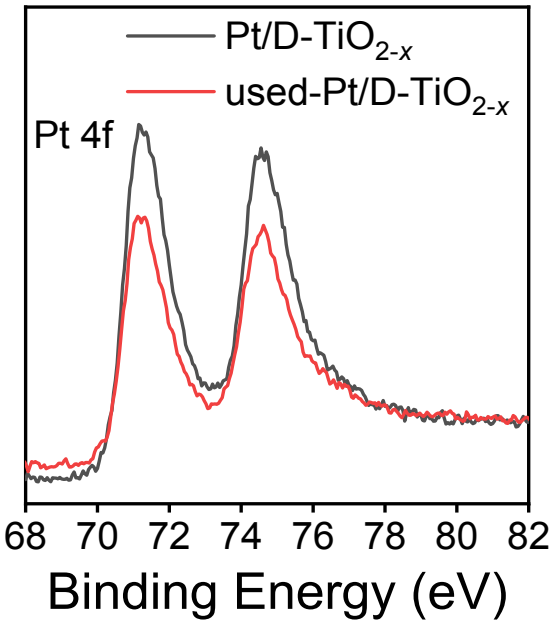

Fig. S16 Pt 4f doublet states in high resolution XPS spectra of Pt/D-TiO_{2-x} and used Pt/D-TiO_{2-x}.

Table S2 Comparison of the selectivity of CH_4 over Pt loaded on different semiconductor catalysts in photoreduction CO_2.

Catalyst	Mass	Reactants	Light Source	Max CH_4 Yield ($\mu mol\ h^{-1}$)	Selectivity of CH_4	Temperature
Pt/TiO_2(AB) in this wok	20 mg	CO_2+H_2O (g)	150 W Xe lamp	**0.3412**	**87.5%**	393 K
[6] Pt/TiO_2(P25) $MgO/Pt/TiO_2$(P25)	20 mg	CO_2+H_2O (g)	100 W Xe lamp	0.104 0.22	37.9% 80%	323 K
[7] Pt/TiO_2	200 mg	CO_2+H_2O (l)	40 W Hg UV lamp	0.7	5.5%	298 K
[8] Pt/TiO_2 Pt-PANI-TiO_2	10 mg	CO_2+H_2O (g)	320-780 nm	0.15 0.5	34.7% 38.5%	298 K
[9] Pt/Ga_2O_3	200 mg	CO_2+H_2O (l)	300 W Xe lamp	1.52	15.3%	298 K
[10] Pt/TiO_2 $CuO/Pt/TiO_2$	20 mg	CO_2+H_2O (l)	300 W Xe lamp	0.0084 0.0284	65.4% 99.1%	293 K
[11] Pt/TiO_2/MgAl	20 mg	CO_2+H_2O (g)	300W Xe lamp	0.364	85.5%	298 K
[12] Pt/In_2O_3	20 mg	CO_2+H_2O (l)	500W Hg lamp	0.054	89.5%	298 K
[1] Pt/TiO_2(B)	10 mg	CO_2+H_2O (g)	300 W Xe lamp	0.664	83.1%	298 K
[13] Pt/C-TiO_2	20 mg	CO_2+H_2O (l)	8W Hg UV lamp	0.037	42.1%	298 K

References

1 Y. Liu, C. Miao, P. Yang, Y. He, J. Feng and D. Li, *Appl. Catal., B*, 2019, **244**, 919–930.

2 G. Yin, X. Huang, T. Chen, W. Zhao, Q. Bi, J. Xu, Y. Han and F. Huang, *ACS Catal.*, 2018, **8**, 1009–1017.

3 G. Yin, Q. Bi, W. Zhao, J. Xu, T. Lin and F. Huang, *ChemCatChem*, 2017, **9**, 4389–4396.

4 L. Wang, Y. Wang, Y. Cheng, Z. Liu, Q. Guo, M. N. Ha and Z. Zhao, *J. Mater. Chem. A*, 2016, **4**, 5314–5322.

5 Z. Zhao, X. Zhang, G. Zhang, Z. Liu, D. Qu, X. Miao, P. Feng and Z. Sun, *Nano Res.*, 2015, **8**, 4061–4071.

6 S. Xie, Y. Wang, Q. Zhang, W. Deng and Y. Wang, *ACS Catal.*, 2014, **4**, 3644–3653.

7 J. Dong, J. Han, Y. Liu, A. Nakajima, S. Matsushita, S. Wei and W. Gao, *ACS Appl. Mater. Interfaces*, 2014, **6**, 1385–1388.

8 G. Liu, S. Xie, Q. Zhang, Z. Tian and Y. Wang, *Chem. Commun.*, 2015, **51**, 13654–13657.

9 Y. X. Pan, Z. Q. Sun, H. P. Cong, Y. L. Men, S. Xin, J. Song and S. H. Yu, *Nano Res.*, 2016, **9**, 1689–1700.

10 Z. Xiong, Z. Lei, C. C. Kuang, X. Chen, B. Gong, Y. Zhao, J. Zhang, C. Zheng and J. C. S. Wu, *Appl. Catal. B*, 2017, **202**, 695–703.

11 R. Chong, C. Su, Y. Du, Y. Fan, Z. Ling, Z. Chang and D. Li, *J. Catal.*, 2018, **363**, 92–101.

12 C. W. Y. Wang, J. Zhao, Y. Li, *Appl. Catal., B*, 2018, **226**, 544–553.

13 M. Tasbihi, M. Schwarze, M. Edelmannová, C. Spöri, P. Strasser and R. Schomäcker, *Catal. Today*, 2019, **328**, 8–14.